Spin-Tagged Electron-Hydrogen Scattering: Ionization in the Near-Threshold Region

X. Q. Guo,[1] D. M. Crowe,[1] M. S. Lubell,[1] F. C. Tang,[1],[a] A. Vasilakis,[1],[b] J. Slevin,[2] and M. Eminyan[3]

[1]*Department of Physics, City College of City University of New York, New York, New York 10031*
[2]*Department of Experimental Physics, St. Patrick's College, Maynooth, Maynooth, Co. Kildare, Ireland*
[3]*Laboratoire de Physique Atomique, Tour 24, Universite Paris VII, F-75251 Paris, France*

(Received 14 December 1989; revised manuscript received 10 August 1990)

We used beams of polarized electrons and polarized hydrogen atoms to measure the ionization-rate asymmetry, $\Delta_I = [R(\uparrow\downarrow) - R(\uparrow\uparrow)]/[R(\uparrow\downarrow) + R(\uparrow\uparrow)]$, in the near-threshold region, where $R(\uparrow\downarrow)$ and $R(\uparrow\uparrow)$ are the ionization rates when the electron spin is antiparallel and parallel, respectively, to the atomic spin. Within 1.7 eV above threshold, our results reveal the presence of structure, which heretofore has not been predicted by any conventional theoretical calculation.

PACS numbers: 34.80.Dp, 34.80.Nz

In the realm of electron-atom scattering, the electron-hydrogen collision system has long served as the principal testing ground for the approximation methods that are used to make electron-atom scattering amenable to theoretical analysis. The deficiencies and strengths of the various theoretical models are illuminated most clearly when comparisons are made with experiments that provide access to the collision system at the most fundamental level, in which scattering observables can be examined unencumbered by averages over momentum, angular momentum, or spin. In this Letter we report new measurements of spin-dependent asymmetries for impact ionization in the 13.6–15.3-eV near-threshold region. We began these studies as a sequel to earlier investigations of impact ionization,[1] which today must be regarded as exploratory in nature as a consequence of the limitations placed on them by the technologies available at the time. The advent of the GaAs polarized-electron source[2] in particular has now enabled us to make a substantial improvement in the quality of the measurements.

As in the earlier work,[1] the quantity of interest is the ionization asymmetry A_I defined by

$$A_I \equiv [\sigma_I(\uparrow\downarrow) - \sigma_I(\uparrow\uparrow)]/[\sigma_I(\uparrow\downarrow) + \sigma_I(\uparrow\uparrow)] , \qquad (1)$$

where $\sigma_I(\uparrow\downarrow)$ and $\sigma_I(\uparrow\uparrow)$ are respectively the total ionization cross section for the antiparallel and parallel spin configurations of the incident and atomic electrons. The quantity actually measured is the experimental counting-rate asymmetry Δ_I defined analogously to A_I with $R(\uparrow\downarrow)$ and $R(\uparrow\uparrow)$, the ion counting rates (normalized to incident electron and atom intensities), replacing $\sigma_I(\uparrow\downarrow)$ and $\sigma_I(\uparrow\uparrow)$. The quantities A_I and Δ_I are related by the expression $\Delta_I = P_e P_H (1 - F_2)|\cos\alpha| A_I$, where P_e and P_H are the polarizations of the electron and hydrogen beams, respectively, F_2 is the fraction of events attributable to hydrogen molecules, and α is the angle between the two polarization vectors. For purposes of relating A_I to Δ_I, these parameters may be taken approximately as follows: $P_e \approx 0.25$, $P_H \approx 0.5$, $F_2 \approx 0$, and $|\cos\alpha| \approx 1$.

Our experiment employed a crossed-beam geometry, as described elsewhere.[3-5] In brief, polarized electrons were produced by photoemission from ⟨100⟩ GaAs with light from a GaAlAs diode laser.[3] The helicity of the electrons extracted from the crystal was controlled by the rotation of either a quarter-wave ($\lambda/4$) or a half-wave ($\lambda/2$) retardation plate in the optics train. A beam flag allowed the light to be blocked periodically for background measurements. Before reaching the interaction region, the extracted beam passed through a set of electron optical elements containing a 90° spherical bender and a 180° hemispherical monochromator. The electron current, which varied between 30 and 150 nA, was monitored by a Faraday cup located just beyond the interaction region.

The polarized atomic-hydrogen beam[4] originated in an rf dissociation source and underwent high-field state selection in a pair of permanent hexapole magnets. Following the magnets, the spins of the hydrogen atoms were rotated adiabatically into the longitudinal direction by a small solenoidal coil. Additional coils maintained the field in the longitudinal direction and trimmed it to the 100 mG required at the crossed-beam interaction site. During the experiment, as a consistency check at several electron energies, we reversed the hydrogen polarization by reversing the direction of the magnetic guide fields. At the end of the line, the beam was sampled by a quadrupole mass analyzer that served as an intensity monitor. At the interaction region the hydrogen beam was characterized[4] by a molecular fraction of 0.05 and a density of $\sim 10^{10}$ atoms/cm^3. When the beam was turned on, the residual gas pressure (N_2 gauge calibrated) rose from $\sim (3 \text{ to } 6) \times 10^{-9}$ Torr.

A channel electron multiplier (CEM), preceded by a grid to prevent electrons or negative ions from reaching the CEM entrance cone, served as an ion detector. The CEM was enclosed in a stainless-steel box that extended upstream to the interaction region and provided 4π acceptance for the recoiling ions. We varied the grid and cone bias voltages to ensure that the signal was free from photon contamination.

We reduced systematic effects by reversing the electron polarization at frequent intervals. To this end, under computer control we rotated the $\lambda/2$ and $\lambda/4$ plates through 360°, the former in eight steps of 45° and the latter in four steps of 90°. During data acquisition, for each data run j, we time ordered the $\lambda/2$- and $\lambda/4$-plate orientations to produce eight helicity sets, each of which contained four circular-polarization settings alternating between left and right. Thus for each run we generated eight sets of data, in each of which the electron and atom polarization vectors alternated between antiparallel and parallel configurations, each appearing twice.

For each of the eight data sets, within a given run j, we calculated a single "real" asymmetry Δ_R^j, as well as two "false" asymmetries $\Delta_{F_+}^j$ and $\Delta_{F_-}^j$, which should be zero in the absence of systematic effects. We calculated Δ_R^j from the average of the rates $R(\uparrow\downarrow)_1^j$ and $R(\uparrow\downarrow)_2^j$ for the two antiparallel configurations and the average of the rates $R(\uparrow\uparrow)_1^j$ and $R(\uparrow\uparrow)_2^j$ for the two parallel configurations. Following procedures similar to those used in the earlier work,[1] we generated the two false asymmetries by taking differences and sums for the antiparallel and parallel configurations in accordance with the prescription

$$\Delta_{F_\pm}^j = \frac{[R(\uparrow\downarrow)_1^j - R(\uparrow\downarrow)_2^j] \pm [R(\uparrow\uparrow)_1^j - R(\uparrow\uparrow)_2^j]}{[R(\uparrow\downarrow)_1^j + R(\uparrow\downarrow)_2^j] + [R(\uparrow\uparrow)_1^j + R(\uparrow\uparrow)_2^j]} . \quad (2)$$

We used the false asymmetries to search for the presence of spurious helicity-correlated effects, experimental noise insufficiently represented by the calculated statistical uncertainties, and tuning drifts of the beams or the electronic instrumentation. By construction, the Δ_{F_+}'s are most sensitive to quasilinear drifts, while the Δ_{F_-}'s are most sensitive to quasiquadratic drifts. Therefore we combined all the Δ_{F_+}'s for all data sets and all data runs (including those described elsewhere[5]), irrespective of energy, to generate the histogram shown in Fig. 1(a). Similarly, we combined all the Δ_{F_-}'s to generate the histogram shown in Fig. 1(b). Consistent with our prior observation that drift-related noise appeared intermittently during data acquisition, we found that to high accuracy we could fit each histogram with the sum of two Gaussians, a dominant one (curve 1) having a narrow width corresponding to "drift-free" operation and a subordinate one (curve 2) having a broad width corresponding to "drift-hindered" operation. We also found that quasilinear drift was more prevalent than quasiquadratic drift, as illustrated by the relative heights of the broad Gaussians in Figs. 1(a) and 1(b).

In order to determine an effective uncertainty for the true distributions given by the histograms, we used a combination of the variances of the individual Gaussians appropriately weighted for such statistical mixing. We then found that all sixteen false asymmetries were very small and statistically consistent with zero with essentially ideal chi-square confidence levels. In order to preclude an accidental bias of our results at any given energy due to small finite sample size, however, we elected to cut our data based upon a truncation of the histograms of Figs. 1(a) and 1(b) at the level of 2.5 standard deviations from zero, a criterion that was satisfied by more than 90% of the data. We thus reduced the contributions of the broad distributions substantially while removing only ~3% of the narrow distributions. Having made the cuts, we found that the calculated variances for the resulting statistical mixtures produced 8% increases in the original uncertainties for both the Δ_{F_+}'s and Δ_{F_-}'s. The false-asymmetry summaries for the truncated data are shown in Fig. 2, demonstrating to extremely high confidence the absence of systematic effects. Taken as a group, the Δ_{F_+}'s average to $+32(24)\times10^{-5}$ and the Δ_{F_-}'s to $-57(24)\times10^{-5}$. Their consistency with zero is further demonstrated by their respective χ_ν^2 values of 1.04 and 0.96 ($\nu=1408$) for assumed values of zero. We therefore conclude that our truncated data are free from systematic effects at the level of approximately $\pm5\times10^{-4}$.

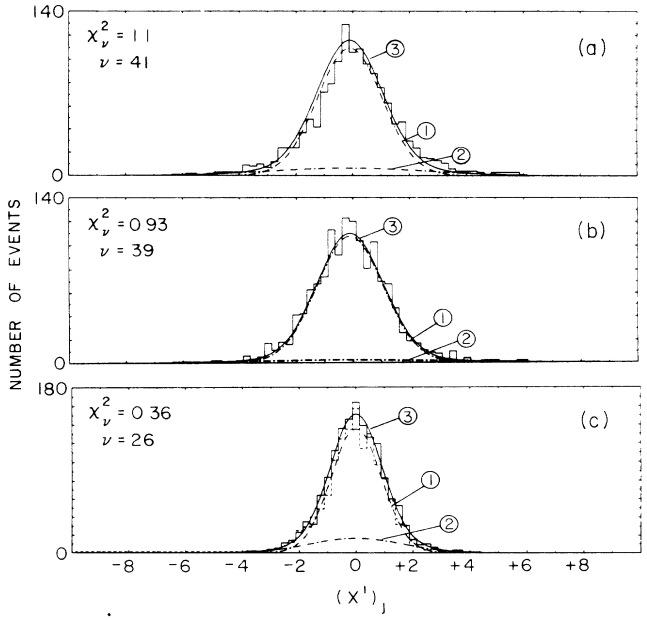

FIG. 1. Analysis of statistical errors: (a) Histogram of normalized false asymmetries, $(x')_j=(\Delta_{F_+}^j)_j/(\sigma_{F_+}^j)_j$, for all data sets i and all runs j, irrespective of energy, where $(\sigma_{F_+}^j)_j$ is the statistical uncertainty for $(\Delta_{F_+}^j)_j$; (b) histogram analogous to that in (a) for Δ_{F_-} false symmetries; (c) histogram (solid) of normalized real-asymmetry residuals, $(x')_j=[(\Delta_R^j)_j-(\bar{\Delta}_R)_j]/(\sigma_R^j)_j$, where $(\bar{\Delta}_R)_j$ is the weighted mean of the real asymmetry for the jth data run, and histogram (dashed) of real-asymmetry residuals for truncated data set as explained in text. In each case the curve labeled 3 is obtained from a fit of the data by the sum of two Gaussians labeled 1 and 2.

We carried out our analysis of the real-asymmetry uncertainties in a manner analogous to that which we used for the false asymmetries. The histogram of real-

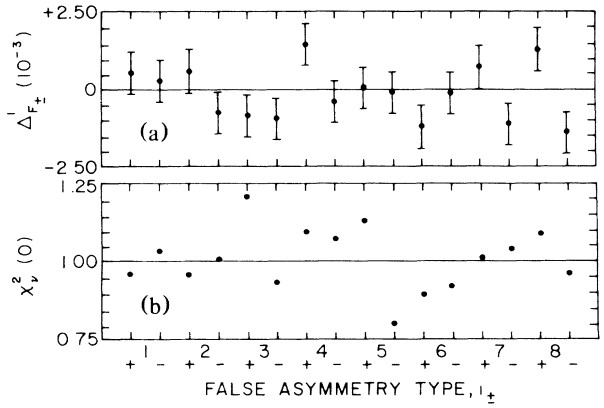

FIG. 2. (a) Summary of the sixteen false asymmetries $\langle \Delta F_{l\pm} \rangle$, each averaged over all runs irrespective of energy. (b) Corresponding set of reduced chi squares $\chi^2_\nu(0)$ for assumed average of zero. The number of degrees of freedom ν varies between 143 and 159.

asymmetry residuals, shown solid in Fig. 1(c), again is extremely well represented by the sum of two Gaussians. After *false-asymmetry* truncation, the real-asymmetry residuals assume the slightly narrower histogram shown dashed in Fig. 1(c). Note that within statistics and binning errors (approximately 0.1 standard deviation), the symmetry of the histogram of the untruncated data is preserved in the histogram of the truncated data, emphasizing the lack of bias introduced by the truncation procedure. From an analysis of the histogram of the truncated data, we found that the original statistical uncertainties had to be increased by a factor of 1.07.

We illustrate the level of stability that we achieved in the experiment by the consistency of the 24 asymmetry measurements shown in Fig. 3 for 15.07 eV, an energy to which we periodically returned during our quasirandom energy sequence in the data-taking procedure. In order to account for the continuing change in the value of the negative electron affinity of the GaAs crystal, we found that it was necessary to calibrate the energy of the electron beam at periodic intervals (25–50 h). Using a molecular-ionization extrapolation method,[3] which led to a typical energy accuracy of ± 30 meV, we observed that during one crystal lifetime ($1/e$ lifetime $\geqq 400$ h), the energy drifted upward by 50–75 meV, a change large enough to require the periodic calibrations but small enough to leave the polarization virtually unchanged.[6] In separate measurements[3] of the atomic ionization rate between 13.67 and 13.87 eV, we determined that our beam was characterized by a Gaussian width ($\pm\sigma$) of ± 75 meV.

In Fig. 4 we present our measurements of Δ_I. Within a small fraction of a standard deviation, the results of the untruncated data set (not shown for clarity) are indistinguishable from those shown for the truncated set. Over the full region investigated (13.6–15.3 eV), our measurements are inconsistent with a linear dependence

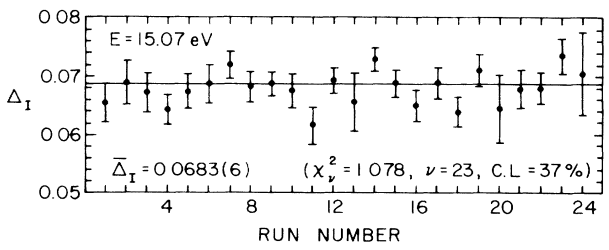

FIG. 3. Stability check showing 24 separate measurements of Δ_I at 15.07 eV.

on energy, as demonstrated by a reduced chi square χ^2_ν of 4.82 for $\nu = 17$ degrees of freedom (confidence level $\sim 5\times10^{-10}$) for such a fit. Structure is clearly evident, with any possible sharp features masked by the ± 75-meV energy spread of the electron beams. (We note that evidence of this structure was already present in less precise preliminary measurements carried out with a different prescription several years ago.)

Near threshold, the Wannier law[7,8] predicts that if the $^3S^e$ and $^1P^e$ final states are ignored, Δ_I should be constant throughout a restricted region, which for hydrogen has been found to extend for about 0.5 eV above threshold.[9] Although our ± 75-meV energy spread makes a precise comparison somewhat problematic, we note that a fit of a constant function to our data within this region results in a χ^2_ν value of 2.32 for $\nu = 6$, corresponding to a marginal confidence level of 3%. A careful analysis of our data,[10] in fact, suggests that, structure aside, within the restricted region 13.6–14.2 eV, Δ_I is characterized by a generally positive slope with respect to increasing ener-

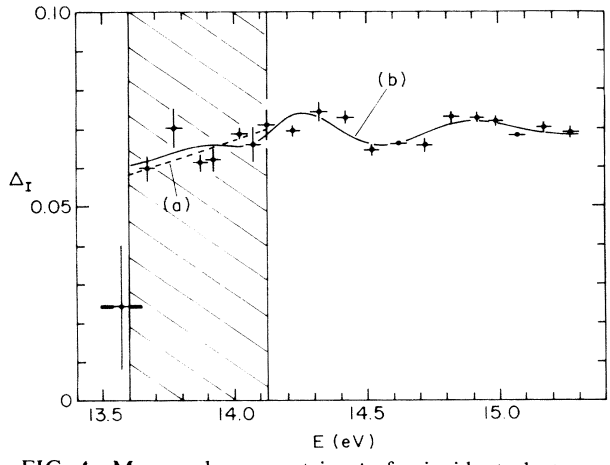

FIG. 4. Measured asymmetries Δ_I for incident electron energies between 13.57 and 15.27 eV. (A table of the values of Δ_I is available from the authors.) The vertical and horizontal error bars represent 1-standard-deviation uncertainties. The heavy, outer error bar on the 13.57-eV point illustrates the characteristic energy spread of the electron beam. Curve *a* is a linear fit in the restricted (hatched) region while curve *b* is an example of a fit (see text) of the Coulomb dipole theory (Ref. 11).

gy. (A linear fit in this region actually produces a χ_ν^2 value of 0.78 for $\nu=5$, corresponding to a confidence level of 56%.)

For completeness we also compare our data to the Coulomb-dipole theory,[11] which by contrast with the Wannier picture predicts rapid oscillations in both the ionization cross section σ_I and the associated asymmetry Δ_I. Although the underlying principles of the Coulomb-dipole theory have remained largely unchanged since Temkin first introduced them, the functional form for σ_I has experienced substantial evolution, and currently the precise form is uncertain. Curve *b* in Fig. 4, which is an eight-parameter convoluted fit of Temkin's latest (unpublished) work, should therefore be regarded only as an illustrative example of the structure present in the Coulomb-dipole model. The poor value of 1.88 for χ_ν^2 ($\nu=11$) may be indicative of deficiencies in the specific model function used or of the inappropriateness of the 1.7-eV range to which it was applied. Additionally, it may reflect our inability to determine an absolute chi-square minimum given the pathology of the function and the limitations of the nineteen-point data set available.

Setting aside the validity of specific threshold laws for the present, we conclude by reemphasizing that our results demonstrate the existence of structure in the ionization asymmetry, which, to the best of our knowledge, has not been predicted by any conventional theoretical calculation. We note that while previous measurements of threshold asymmetries in the alkali metals[12] did not reveal any similar structure, the energy scale for such effects might be smaller for the alkali metals, making such experiments less sensitive, given the energy spread and especially the energy drift of GaAs polarized electron beams. By contrast, high-resolution studies of the absolute two-electron photoionization cross sections of H^- and K^- provided some suggestions of structure,[13] although in each case, within the statistical accuracy of the measurements the results were found to be in satisfactory agreement with the Wannier power law as well.

We wish to acknowledge the financial support of the U.S. NSF, the Research Foundation of City University of New York, NATO, the United Kingdom Science and Engineering Research Council, St. Patrick's College, and the French CNRS. We also wish to thank Professor P. A. Souder, Professor M. R. Frankel, Dr. A. Temkin, Professor A. R. P. Rau, and Professor K. MacAdam for several useful discussions.

---

[a]Present address: Department of Physics, Rice University, P.O. Box 1892, Houston, TX 77251.

[b]Present address: Frequency Electronics, Uniondale, Long Island, NY 11553.

[1]G. D. Fletcher *et al.*, Phys. Rev. A **31**, 2854 (1985), and references therein; T. J. Gay *et al.*, Phys. Rev. A **26**, 3664 (1982); M. J. Alguard *et al.*, Phys. Rev. Lett. **39**, 334 (1977).

[2]See, for example, D. T. Pierce *et al.*, Rev. Sci. Instrum. **51**, 478 (1980), and references therein.

[3]F. C. Tang *et al.*, Rev. Sci. Instrum. **57**, 3004 (1986); X. Q. Guo *et al.*, Rev. Sci. Instrum. **61**, 1858 (1990).

[4]N. Chan *et al.*, Z. Phys. D **10**, 393 (1988).

[5]D. M. Crowe *et al.*, J. Phys. B **23**, L325 (1990).

[6]H.-J. Drouhin *et al.*, J. Phys. (Paris), Lett. **44**, L1027 (1983).

[7]G. H. Wannier, Phys. Rev. **90**, 817 (1953).

[8]A. R. P. Rau, Phys. Rev. A **4**, 207 (1971); R. Peterkop, J. Phys. B **4**, 513 (1971); T. A. Roth, Phys. Rev. A **5**, 476 (1971); H. Klar and W. Schlecht, J. Phys. B **9**, 1699 (1976); H. Klar, J. Phys. B **14**, 3255 (1981); C. H. Greene and A. R. P. Rau, Phys. Rev. Lett. **48**, 533 (1983); J. Phys. B **16**, 99 (1983).

[9]J. W. McGowan and E. W. Clarke, Phys. Rev. **167**, 43 (1968).

[10]With photon contamination absent, the theoretical predictions for field ionization of Rydberg atoms [T. F. Gallagher, Rep. Prog. Phys. **51**, 143 (1988)] in the vicinity of the detector leads us to conclude that the event rate at the "subthreshold" 13.57-eV data point (not used in any of our fits) must have been heavily dominated by impact ionization produced by the high-energy tail of the electron distribution lying within ~ 50 meV of threshold. The value of Δ_I at 13.57 eV is thus consistent with the generally positive slope of $\Delta_I(E)$ at threshold, particularly since the actual value at 13.57 eV must be slightly lower than that shown, given the higher polarization associated with the high-energy tail of GaAs photoelectrons (cf. Ref. 6).

[11]A. Temkin, Phys. Rev. Lett. **16**, 835 (1966); **49**, 365 (1982); J. Phys. B **7**, L450 (1974); IEEE Trans. Nucl. Sci. **30**, 1106 (1983); Phys. Rev. A **30**, 2737 (1984); A. Temkin and Y. Hahn, Phys. Rev. A **10**, 708 (1974); A. Temkin (private communication).

[12]M. H. Kelley *et al.*, Phys. Rev. Lett. **51**, 2191 (1983); G. Baum *et al.*, J. Phys. B **18**, 531 (1985).

[13]J. B. Donahue *et al.*, Phys. Rev. Lett. **48**, 1538 (1982); Y. K. Bae and J. R. Peterson, Phys. Rev. A **37**, 3254 (1988).